

Manuscript Number:

Title: The Effect of Bacterial Growth Phase and Culture Concentration on U(VI) Removal from Aqueous Solution

Article Type: Research paper

Keywords: bacteria; uranium; growth phase; FT-IR; radioactive waste disposal

Corresponding Author: Dr. Janice Kenney,

Corresponding Author's Institution: Imperial College London

First Author: Janice Kenney

Order of Authors: Janice Kenney; Tim Ellis; Felix Nicol; Alex Porter; Dominik Weiss

Abstract: Bacteria play a key role in controlling the mobility of contaminants, such as uranium (U), in the environment. Uranium could be sourced from disposed radioactive waste, derived either from surface disposal trenches for Low Level Waste (LLW) that, because of the waste type and disposal concept, would typically present acidic conditions (both aerobic and anaerobic), or from the geological disposal of LLW or Intermediate Level Waste (ILW) that, because of the waste type and the disposal concept, would typically present alkaline conditions (anaerobic only). In disposed radioactive waste, there could be variable amounts of cellulosic material. Bacterial cells may be living in a range of different growth phases, depending on the growth conditions and nutrients available at the time any waste-derived U migrated to the cells. A key knowledge gap to date has been the lack of a mechanistic understanding of how bacterial growth phases (exponential, stationary, and death phase) affect the ability of bacteria to remove U(VI) from solution. To address this, we first characterised the cells using potentiometric titrations to detect any differences in proton binding to proton active sites on *Pseudomonas putida* cells at each growth phase under aerobic conditions, or under anaerobic conditions favourable to U(IV) reoxidation. We then conducted batch U(VI) removal experiments with bacteria at each phase suspended in 1 and 10 ppm U aqueous solutions with the pH adjusted from 2-12 as well as with culture concentrations from 0.01 - 10 g/L, to identify the minimal concentration of bacteria in solution necessary to affect U removal. We found that, in death phase, *P. putida* cells exhibited double the concentration of proton active sites than bacteria grown to exponential and stationary phase. However, we did not see a difference in the extent of U(VI) removal, from a 10 ppm U solution, between the different growth phases as a function of pH (2 to 12). Culture concentration affected U removal between pH 2-8, where U removal decreased with a decreasing concentration of cells in solution. When the pH was 10-12, $\leq 55\%$ of U precipitated abiotically. The presence of bacteria in solution (0.01 - 10 g/L), regardless of growth phase, increased the precipitation of U from $\leq 55\%$ up to 70-90%, accumulating inside the cells and on the cell walls as $\sim 0.2 \mu\text{m}$ uranyl phosphate

precipitates. These precipitates were also found at low pH with the exception of cells at exponential growth phase. This study demonstrates that growth phase affects the proton-active site concentration but not the extent of U bound to *P. putida* cells and that growth phase dictates the form of U removed from solution. Since the pH of trench-disposed LLW is controlled by the degradation of cellulosic waste, leading to acidic conditions (pH 4-6), bacterial concentrations would be expected to highly affect the extent of U removed from solution. The cement in grouted ILW and LLW, for geologic disposal, will allow for the development of extremely high pH values in solution (pH 9-13), where even the smallest concentrations of bacteria were able to significantly increase the removal of U from solution under aerobic conditions, or under anaerobic conditions favourable to U(IV) reoxidation.

Suggested Reviewers: Shannon Flynn
Newcastle University
shannon.flynn@newcastle.ac.uk

Michael Hochella
Virginia Tech
hochella@vt.edu

Bryne Ngwenya
University of Edinburgh
Bryne.Ngwenya@ed.ac.uk

Katherine Morris
University of Manchester
katherine.morris@manchester.ac.uk

Department of Earth Science and Engineering,
Imperial College London

Imperial College
London

London SW7 2AZ, UK
Telephone: +44 (0)77 5219 5974

August 17th, 2017

Professor Jeremy B. Fein
University of Notre Dame,
Notre Dame, IN, 46556

Dear Professor Fein,

Please find submitted for your consideration a research article entitled “The Effect of Bacterial Growth Phase and Culture Concentration on U(VI) Removal from Aqueous Solution” for publication in *Chemical Geology*. My co-authors are aware of and concur with its submission. This work has not been published previously, there are no conflicts of interest, nor is it under consideration by another journal. We acknowledge funding for this project came from the Natural Environment Research Council, Radioactive Waste Management Limited, and Environment Agency for the funding received for this project through the Radioactivity and the Environment (RATE) programme.

One of the key questions in radioactive waste disposal is understanding how microbial life will affect the waste after it escapes its engineered barriers. Due to variable amounts of cellulosic material (i.e. carbon source) embedded in cemented wastes, bacterial cells may be living in a range of different growth phases at the time any waste-derived U migrated to the cells. Therefore, we investigated how growth phase (exponential, stationary, and death phase) and culture concentration (10g/L – 0.01 g/L) of *P. putida* affected the removal of U from solution in the pH range between 2 and 12, under aerobic conditions. To do this we first characterised how the bacterial cells changed as a function of growth phase, using surface complexation modelling of potentiometric titration data and interpretation of FT-IR spectroscopy from cells from those titrations. We found that the cells at death phase had significantly more EPS than those at exponential and stationary phases, wherefore we expected more U immobilization via death phase cells. We instead found that cells of all growth phases removed a similar extent of U from solution.

The most interesting finding was that growth phase had a significant affect on how U was removed form solution. The cells precipitated U as a uranyl phosphate mineral, either in the cell wall (at pH 5) or within the cell (pH 11), with the exception of cells at exponential phase at pH 5, where cells adsorbed the U. Therefore, the mechanism of U immobilisation may change drastically depending on the growth phase of the bacteria in solution.

Thank you for your consideration of this work,

J. P.L. Kenney, T. Ellis, F. Nicol, A. Porter, and D. J. Weiss

Janice P. L. Kenney

1 **The Effect of Bacterial Growth Phase and Culture Concentration on U(VI) Removal**
2 **from Aqueous Solution**

3 Janice P. L. Kenney¹, Tim Ellis², Felix S. Nicol¹, Alexandra Porter², and Dominik J. Weiss¹

4 1-Department of Earth Science and Engineering, Imperial College London, London, United
5 Kingdom

6 2-Department of Materials, Imperial College London, London, United Kingdom

7 **Abstract**

8 Bacteria play a key role in controlling the mobility of contaminants, such as uranium (U), in
9 the environment. Uranium could be sourced from disposed radioactive waste, derived either
10 from surface disposal trenches for Low Level Waste (LLW) that, because of the waste type
11 and disposal concept, would typically present acidic conditions (both aerobic and anaerobic),
12 or from the geological disposal of LLW or Intermediate Level Waste (ILW) that, because of
13 the waste type and the disposal concept, would typically present alkaline conditions
14 (anaerobic only). In disposed radioactive waste, there could be variable amounts of cellulosic
15 material. Bacterial cells may be living in a range of different growth phases, depending on the
16 growth conditions and nutrients available at the time any waste-derived U migrated to the
17 cells. A key knowledge gap to date has been the lack of a mechanistic understanding of how
18 bacterial growth phases (exponential, stationary, and death phase) affect the ability of
19 bacteria to remove U(VI) from solution. To address this, we first characterised the cells using
20 potentiometric titrations to detect any differences in proton binding to proton active sites on
21 *Pseudomonas putida* cells at each growth phase under aerobic conditions, or under anaerobic
22 conditions favourable to U(IV) reoxidation. We then conducted batch U(VI) removal
23 experiments with bacteria at each phase suspended in 1 and 10 ppm U aqueous solutions with
24 the pH adjusted from 2-12 as well as with culture concentrations from 0.01 - 10 g/L, to

25 identify the minimal concentration of bacteria in solution necessary to affect U removal. We
26 found that, in death phase, *P. putida* cells exhibited double the concentration of proton active
27 sites than bacteria grown to exponential and stationary phase. However, we did not see a
28 difference in the extent of U(VI) removal, from a 10 ppm U solution, between the different
29 growth phases as a function of pH (2 to 12). Culture concentration affected U removal
30 between pH 2-8, where U removal decreased with a decreasing concentration of cells in
31 solution. When the pH was 10-12, $\leq 55\%$ of U precipitated abiotically. The presence of
32 bacteria in solution (0.01 – 10 g/L), regardless of growth phase, increased the precipitation of
33 U from $\leq 55\%$ up to 70-90%, accumulating inside the cells and on the cell walls as $\sim 0.2 \mu\text{m}$
34 uranyl phosphate precipitates. These precipitates were also found at low pH with the
35 exception of cells at exponential growth phase. This study demonstrates that growth phase
36 affects the proton-active site concentration but not the extent of U bound to *P. putida* cells
37 and that growth phase dictates the form of U removed from solution. Since the pH of trench-
38 disposed LLW is controlled by the degradation of cellulosic waste, leading to acidic
39 conditions (pH 4-6), bacterial concentrations would be expected to highly affect the extent of
40 U removed from solution. The cement in grouted ILW and LLW, for geologic disposal, will
41 allow for the development of extremely high pH values in solution (pH 9-13), where even the
42 smallest concentrations of bacteria were able to significantly increase the removal of U from
43 solution under aerobic conditions, or under anaerobic conditions favourable to U(IV)
44 reoxidation.

45 **1.0 Introduction**

46 Radionuclides can be released into the environment *via* the degradation of radioactive waste
47 disposal containers and the evolution of their associated wastefrom. The release of
48 radionuclides, such as uranium (U), from low- and intermediate-level waste (LLW and ILW,
49 respectively) containers will occur under different pH environments, depending on the means

50 and location of disposal. Historically, disposal of LLW was made to trenches at the Low
51 Level Waste Repository (LLWR) in the UK, where the combination of the corrosion of metal
52 containers and the degradation of cellulosic wastes has led to mildly acidic pH conditions
53 (Cummings and Raaz, 2011). Current and future disposal of grouted LLW and plans for
54 future geologic disposal of ILW, which will be grouted and backfilled with cement, would
55 allow for the development of very alkaline solution (pH 9-13; Francis et al., 1997; Cummings
56 and Raaz, 2011). LLW and ILW may be in an aerobic environment during on-site storage, the
57 operation phase, and the early stages of post-closure, and therefore it is important to
58 understand how U will behave under both pH regimes under aerobic conditions.
59 Additionally, under geologic disposal conditions which contain bicarbonate, along with Fe or
60 Mn, U(IV) may be reoxidized to U(VI) in anaerobic solutions (Wan et al., 2005). Outside the
61 geochemically disturbed near-field zone there will be sharp geochemical gradient to the pre-
62 existing natural conditions of the host rock, and thereby a need to understand the behaviour of
63 radionuclides across of range of geochemical conditions.

64 Bacteria are ubiquitous in the environment, persisting in rock bodies beneath the earth's
65 surface (Pedersen and Ekendahl, 1990), and would therefore be inevitably found in the near-
66 field environment of radioactive waste disposal sites as well as within the sites as introduced
67 via geologic disposal facility (GDF) construction, operation, and from the waste itself. Due to
68 the variability of waste materials disposed of in LLW and ILW, the concentration of
69 cellulosic material available to be solubilised would also be variable (Bourbon and Toulhoat,
70 1996). Aqueous organic matter dissolved from the waste would be a nutrient source for the
71 bacteria, acting as a carbon source for bacterial growth and therefore bacterial growth phase
72 may vary throughout a disposal site. Respective bacteria populations may be living in a
73 variety of growth phases when waste-derived U migrates from the disposal wastefrom and
74 interacts with the evolving natural system, depending on the influx of carbon sources to the

75 system, from exponential growth, to stationary phase, to death phase, where stationary or
76 death phase may persist in aqueous environments for long periods of time. Microorganisms
77 undergo varying physiological processes resulting in various exudates and cell wall protein
78 expression as a function of changing growth phase. Currently there is little information
79 available concerning how the various growth phases may affect the ability of bacteria to
80 adsorb or precipitate uranium across the pH ranges relevant to radioactive waste disposal.

81 In bacteria-free systems, U would tend to adsorb to rocks and minerals below pH 9. Above
82 pH 9, U would tend to precipitate abiotically, as a sodium uranium mineral, in solutions rich
83 in NaCl (e.g. Bots et al., 2014; Kenney et al., 2017), but it is unclear what role bacteria will
84 play in such higher pH environments as could be associated with some radioactive waste
85 disposal concepts. Previous studies have shown that bacteria undergo varying physiological
86 processes during growth, which can result in various exudates and cell wall protein
87 expression as a function of changing growth phases (e.g. Gad et al., 2004; Azam et al., 1999;
88 Rolfe et al., 2012; Liu et al., 2016). Limited information is available concerning how
89 bacterial surface properties change as a function of growth phase, and the information that is
90 available shows that the site density of functional groups on the cell surface or associated
91 with bound capsular extracellular polymeric substance (EPS) may be higher at exponential
92 phase or death phase, depending on whether the cells are Gram-positive or Gram-negative.
93 Daughney et al. (2011) performed surface complexation modelling on the cells of *Bacillus*
94 *subtilis*, a Gram-positive bacterium, during exponential and stationary phase to determine the
95 acidity constants of the sites available for binding and the concentration of those sites on the
96 bacterial cell surface. They found that exponential phase bacteria had higher acidity constants
97 and site concentrations than those at stationary phase. The exponential phase bacteria in that
98 study, having more sites available for metal-binding, removed more Cd and Fe from solution
99 than the stationary phase. Liu et al. (2016) studied the effect of growth phase on the surface

100 properties of *Synechococcus* cyanobacterium, a Gram-negative bacterium, and found little
101 differences between acidity constants derived from modelling the titrations of the cells, but
102 did find that cells in death phase had significantly higher concentrations of EPS associated
103 with the cell surface that was produced at death phase. An increase in EPS produced during
104 bacterial growth may lead to increased sites available for immobilising metals, such as U,
105 however several studies have not seen a difference in the proton active sites when comparing
106 cells with and without their EPS removed (Ueshima et al., 2008; Kenney and Fein 2011).
107 Increased EPS may also increase the propensity for bacteria to adhere to a rock surface and
108 thereby reduce its environmental mobility (Hong et al., 2013).

109 The adsorption of aqueous U(VI) onto bacterial cells has been examined in detail on bacteria
110 in stationary growth phase and at pH values less than 9 (Fowle et al., 2000; Gorman-Lewis et
111 al., 2005; Sheng et al., 2011; Alessi et al., 2014). Bacteria under those conditions remove
112 nearly 100% of U at circumneutral pH values and greater than 20% removal at pH values as
113 low as pH 1.5 (Fowle et al., 2000; Gorman-Lewis et al., 2005). Gorman-Lewis et al. (2005)
114 also noticed that U adsorption decreased with decreasing concentration of cells in solution.
115 At higher pH values associated with cementitious LLW and ILW disposal (pH > 9), we
116 predict that U would precipitate abiotically, as has been seen by Kenney et al., 2017, but it is
117 unclear whether bacteria would enhance or inhibit precipitation at those pH values.

118 The aim of this study was to understand how growth phase and culture concentration affect
119 the ability of bacterial cells to remove uranium from solution. To achieve this, we first
120 studied how growth phase affected the surface properties of the bacterium *Pseudomonas*
121 *putida*, a microbe found both in soils and in the subsurface. This was done by using surface
122 complexation modelling of potentiometric titrations to determine the acidity constants and
123 site concentration of functional groups on the cells surface and to identify any changes as a
124 function of growth phase. This was complemented with Fourier Transform infrared (FT-IR)

125 spectroscopy on the cells from different growth phases with varying pH, to identify proton
126 active functional groups available for binding. We then conducted batch U removal
127 experiments as a function of pH, growth phase, and culture concentration. Cells incubated
128 with and without U were analysed using FT-IR spectroscopy to elucidate which functional
129 groups were responsible for U removal from solution. In order to confirm if the U-bacteria
130 complexes observed using FT-IR spectroscopy formed due to adsorption or precipitation and
131 to identify the composition of the precipitates, transmission electron microscopy (TEM)
132 combined with energy dispersive x-ray spectroscopy (EDX) were used to generate spatially
133 resolved elemental maps of the mineral precipitates within the cells.

134 **2.0 Material and Methods**

135 **2.1 Bacterial Growth**

136 Cells of *P. putida* were cultured aerobically at 37°C in 10 mL of Luria-Bertani medium and
137 incubated for 24 h. The biomass was transferred to 1 L of the same growth medium and
138 incubated for enough time to bring them to the desired growth phase (exponential, stationary,
139 and death phase). Cells were harvested at 8 h for exponential phase, 24 h for stationary
140 phase, and 96 h for death phase. Each phase was monitored using optical density at 540 nm
141 using a UV-vis spectrometer, with bacteria-free medium as a background to gauge growth.

142 After incubation, the biomass was separated from the growth media via centrifugation at
143 4000 rpm and washed (Kenney and Fein, 2011). Briefly, cells were rinsed 5 times with a
144 clean 0.1 M NaCl electrolyte solution to remove all growth media from the cells so any
145 possible growth would be retarded. After the washing procedure the cells were centrifuged
146 twice at 4000 rpm for 30 minutes, removing as much solution as possible, in order to
147 determine the wet mass of the bacterial pellet to be used in potentiometric titrations and U
148 batch experiments. All further discussion of mass will refer to the wet mass of bacterial cells.

149 **2.2 Potentiometric Titrations**

150 Potentiometric titrations were conducted on suspensions of bacteria (30-50 g/L). The ionic
151 strength of the suspensions was buffered using 0.1 M NaCl, and conducted under an N₂
152 atmosphere. The electrolyte was bubbled with N₂ for 60 minutes prior to suspension, in order
153 to purge atmospheric CO₂. Titrations were carried out a minimum of three times with
154 different cell suspensions, using a Metrohm 888 Titrande automated burette assembly and pH
155 measurements were conducted with an SLS Electrode semi micro glass combination
156 electrode filled with 0.1 M NaCl. The suspensions were first acidified to pH ~2.5 using 1.0 M
157 HCl. Aliquots of 1.0 M NaOH were used to raise the pH of the suspensions up to
158 approximately pH 9.5 before being lowered back down to pH 3 using 1.0 M HCl, to test the
159 reversibility of proton binding. Each individual suspension was stirred throughout the
160 titration with a magnetic stir bar.

161 **2.3 Batch Uranium Removal Experiments**

162 Batch experiments were conducted by measuring the change in aqueous U concentration that
163 occurred upon exposure of an aqueous U solution to the washed *P. putida* cells. A parent
164 solution containing approximately 10 ppm U in 0.1 M NaCl was prepared from a 1000 ppm
165 U standard reference solution. A pellet of washed cells was suspended in the 10 ppm U
166 solution to achieve a bacterial concentration of 1 g/L in each experiment. The parent
167 suspensions were divided into 5 mL volumes in 15 mL polypropylene test tubes, and the
168 solution pH of each suspension was adjusted to a desired starting pH, ranging from pH values
169 of 3 to 12, using small aliquots of 0.1 to 1 M HCl or NaOH. The systems were allowed to
170 equilibrate via end-over-end rotation at 24 rpm for 2 h to allow time for equilibration between
171 the U and the cells. After equilibration the final pH was measured and the cells were
172 separated from the solution via centrifugation at 4000 rpm and then the supernatant was

173 filtered through a 0.45 μm disposable nylon filter. The final concentration of U remaining in
174 solution was determined using inductively coupled plasma-mass spectroscopy (ICP-MS) with
175 matrix-matched standards. The concentration of U removed from solution by the cells was
176 calculated by the difference between the initial and final U concentrations. The pH of the
177 samples was measured before and after equilibration to identify possible drifts in hydrogen
178 concentration.

179 **2.4 Electron Microscopy**

180 TEM (JEOL 2100 Plus) was used to establish whether U is removed *via* adsorption or
181 precipitation, and to determine whether this mechanism changed as a function of growth
182 phase. EDX spectroscopy was used to provide elemental information of cellular precipitates
183 within different growth phases. The exposed cells were pelleted and fixed with 2.5%
184 glutaraldehyde (Sigma) and stained with 1% osmium tetroxide (TAAB) for 30 minutes. Cells
185 were serially dehydrated in a graded ethanol series (50%, 70%, 95% ethanol to ultrapure
186 water) and 100% dried ethanol for 5 minutes each at respective stage before immersing
187 samples in acetonitrile (Sigma) for 15 minutes. Samples were progressively infiltrated with a
188 Quetol-based resin (TAAB) (8.75 g Quetol, 13.75 g nonenyl succinic anhydride, 2.5 g methyl
189 acid anhydride, 0.62 g benzyl dimethylamine) for three days at 50%, 75% and 100%
190 respectively, using acetonitrile diluent. Fresh resin was applied before placing samples under
191 vacuum for 24 hours. Further fresh resin was applied before curing for 4 days at 60°C. Thin
192 sections (70 nm) were cut directly into an aqueous reservoir using an ultramicrotome (RMC
193 products) with a diamond knife set at a wedge angle of 35°. Sections were immediately
194 collected on bare, 300 mesh copper TEM grids (Agar Scientific), dried and coated with 5 nm
195 carbon (PECSII, Gatan). Samples were imaged and analysed in an FEI Titan 80–300
196 scanning/transmission electron microscope (S/TEM) operated at 80 kV, fitted with Cs

197 (image) corrector and SiLi EDX spectrometer (EDAX, Leicester UK). EDX maps were
198 obtained over an area of 88.6 μm^2 , using pixel sizes of 2 nm and dwell times of 16 μs per
199 pixel. EDX data was processed using ESPRIT software (Bruker).

200 **2.5 Fourier Transform Infrared Spectroscopy**

201 FT-IR spectroscopy was conducted on a Nicolet 5700 Spectrometer using a diamond
202 attenuated total reflection (ATR) accessory. Bacterial pellets with and without U at various
203 pH values were pressed onto the ATR crystal and 128 scans were averaged for each sample
204 following a background spectrum of 128 scans with a spectral resolution of 4 cm^{-1} . Spectra
205 of the supernatant were recorded so that the aqueous supernatant spectra could be subtracted
206 from that of the wet bacterial pellet to ensure the entire signal is coming from the U
207 associated with the bacterial cells. All spectra were baseline corrected using asymmetric least
208 squares fitting (Eilers, 2004) with parameters $\lambda = 30,000$ and $p = 0.001$, smoothed using a
209 Savitzky–Golay filter (Savitzky and Golay, 1964) and area-normalised to the amide II band at
210 1548 cm^{-1} (Leone et al., 2007) using a previously developed script (Felten et al., 2015).

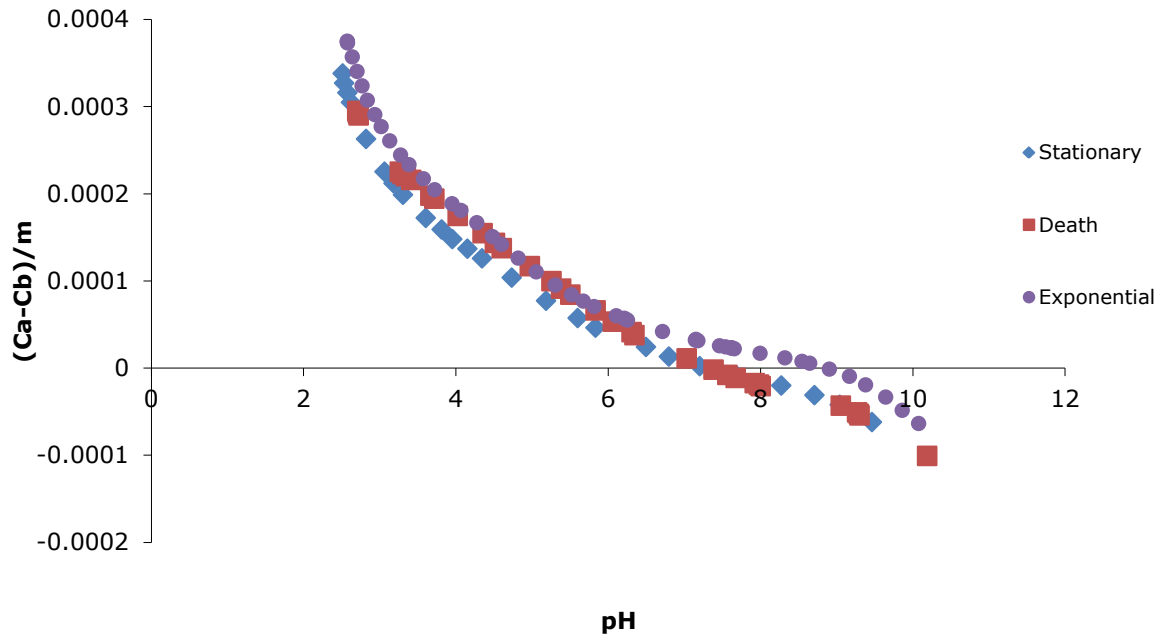
211 **3.0 Results and Discussion**

212 **3.1 Characterisation of bacterial cells at various growth phases**

213 Potentiometric titrations were conducted in triplicate and a representative titration curve is
214 shown in Figure 1. The titrations are plotted as acid and base added during the titration:

$$215 \quad (C_a - C_b)/m \quad (1)$$

216 where C_a and C_b are the total concentrations of acid and base (mol/L) added at each step of
217 the titration and m is the mass (g) of bacterial cells in suspension. The bacteria at all growth
218 phases studied exhibit significant and continuous proton buffering over the entire pH range
219 considered (Figure 1).



220

221 **Figure 1: Potentiometric titration data for *P. putida* (30–50 g/L wet mass) biomass at**
 222 **Stationary (◇), Death (□), and exponential phases (○) in 0.1 M NaCl electrolyte**
 223 **solution. Each curve depicts a representative titration curve generated from triplicate**
 224 **titrations.**

225

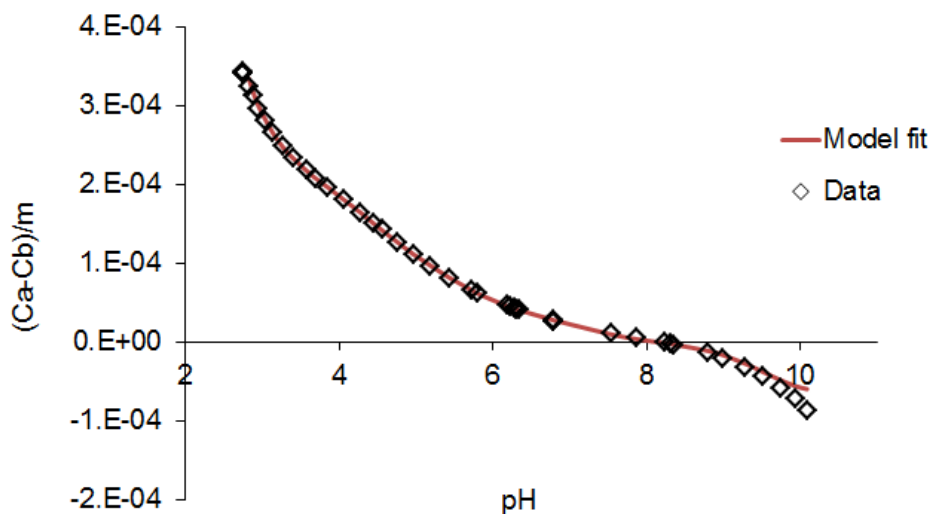
226 Titration data for each titration for the three growth phases studied here were modelled using
 227 a discrete proton-active site surface complexation model, following the approach of Fein et
 228 al. (2005). The functional groups on bacterial cell walls are represented by distinct sites that
 229 deprotonate according to the following reaction:



231 where R represents the bacterial cell wall macromolecules to which each type of functional
 232 group, Site_x, is attached. The equilibrium constant (K_a) for this reaction is expressed as:

233
$$K_a = [\text{R-Site}_x^-][\text{H}^+] / [\text{R-Site}_x\text{H}^\circ] \quad (3)$$

234 where $[R\text{-Site}_x^-]$ and $[R\text{-Site}_x\text{H}^0]$ represent the concentrations of the deprotonated and
 235 protonated form of site type Site_x , respectively, and $[H^+]$ represents the concentration of
 236 protons in solution. Experimental data for proton sorption to the bacterial cells were modelled
 237 with a non-electrostatic surface complexation model. This model has been used to describe
 238 the proton active sites of bacterial cells (Yee and Fein, 2001; Borrok and Fein, 2005; Johnson
 239 et al., 2007; Ueshima et al., 2008).



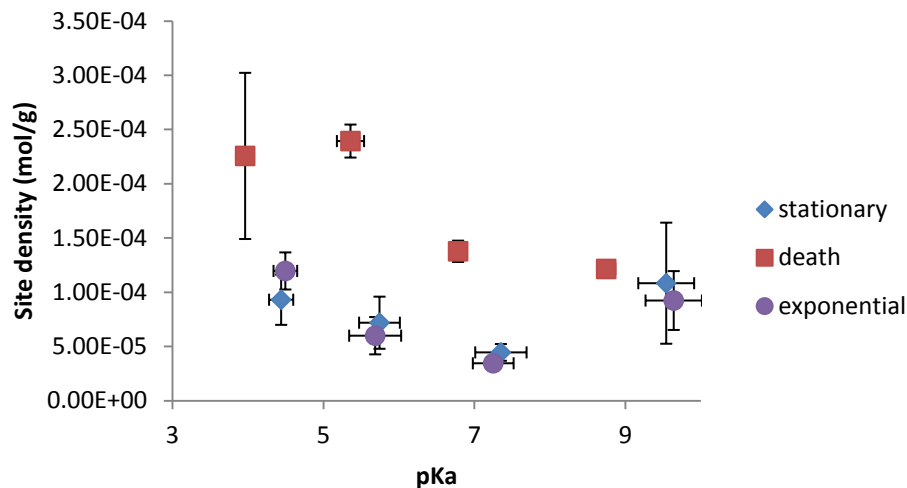
240

241 **Figure 2: A representative example of the goodness of fit of the non-electrostatic model**
 242 **(red curve) to the potentiometric titration data (open diamonds) for *P. putida* cells at**
 243 **exponential phase.**

244 We determined the total number of discrete sites necessary to account for the observed
 245 buffering capacity using FITEQL 2.0 (Westall, 1982). This was done by sequentially testing
 246 models with 1 through 5 proton-active site types until the best fit to the data was determined,
 247 with the goodness of fit for each model being quantified using the residual function in
 248 FITEQL 2.0, $V(Y)$, where the ideal value of 1 characterizes the ideal fit of the model to the
 249 data (Westall, 1982). For each titration modelled here, a four-site model provides the best fit
 250 to the data. The 4-site models consistently yield the $V(Y)$ values closest to 1 (average $V(Y)$

251 of 2.24), as well as the best visual fits to the data for each titration. A representative model fit
 252 to the data is presented in Figure 2.

253



254

255 **Figure 3: pKa values and their corresponding site concentrations for *P. putida* cells at**
 256 **exponential, stationary, and death phases. Error bars represent ± 1 standard deviation**
 257 **from a minimum of three titrations.**

258 The resulting calculated site concentrations and acidity constants are compiled in Figure 3.

259 We find that the pKa values for each of the growth phases in our study were similar, only

260 death phase cells having pKa values lying slightly lower than exponential and stationary

261 phase. Death phase cells had at least 1σ higher site concentrations for the first three sites,

262 with 3σ higher for the second site, and 2σ higher for the third site than the exponential and

263 stationary cells. The pKa values and site concentration from our experiments were all within

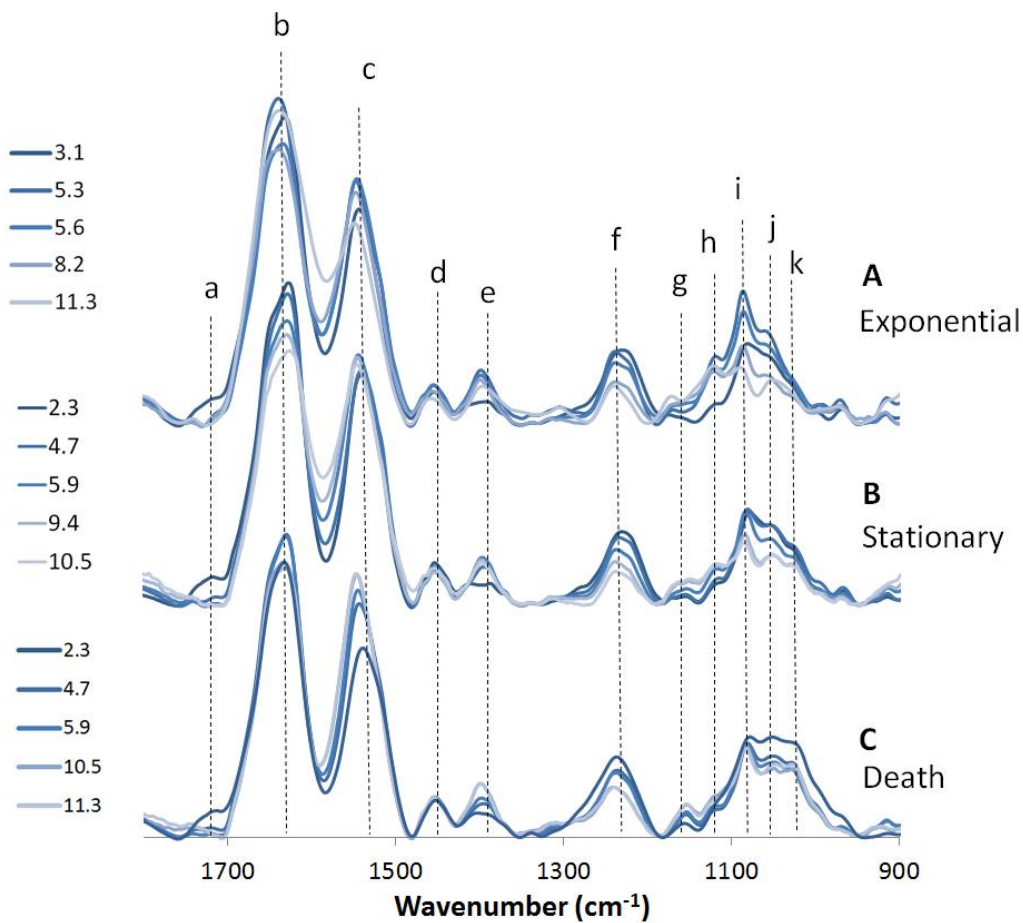
264 2σ of those seen by others for a wide range of bacteria (Johnson et al., 2007; Kenney and

265 Fein, 2011) with the exception of the concentration of proton active sites for the death phase

266 cells in our study were higher than those of the other studies. This trend of higher site

267 densities in death phase from *P. putida*, a Gram-negative species, is the opposite as was seen

268 in Daughney et al. (2001) for the Gram-positive *Bacillus subtilis*, but similar to what was
 269 seen for other Gram-negative species (Liu et al. 2016). This may be due to the fact that
 270 Gram-positive and Gram-negative cells exude EPS differently (Green and Mecsas, 2016),
 271 and therefore in our study the excess of sites in death phase could relate to an increase in cell-
 272 bound EPS. *Pseudomonas* cells have been shown to produce increased amounts of the
 273 polysaccharide alginate with decreasing carbon source and increasing growth (Conti et al.,
 274 1994) and therefore this is likely to be the polysaccharide responsible for the excess site
 275 concentration in death phase cells.



276

277 **Figure 4: Area normalized FT-IR spectra of *P. putida* cells as a function of pH (dark**
 278 **blue to light blue shows transition from pH 2.3 to 11.3) for A) exponential, B)**
 279 **stationary, and C) death phase cells.**

280 FT-IR spectroscopy was conducted on bacterial samples as a function of pH from 2.3-11.3 to
 281 determine how the functional groups of the cells change and to establish whether an increase
 282 in EPS was responsible for the increase in proton active sites in bacteria at death phase.
 283 While FT-IR spectroscopy measures all bonds in the bacterial cells, the active functional
 284 groups are those bands that change with changing pH. The FT-IR spectra of cells at
 285 exponential, stationary, and death phase is shown in figure 4 and the chemical assignment of
 286 each band is given in Table 1. Exponential, stationary, and death phase all exhibited distinct
 287 peaks that correspond to carboxyl, phosphoryl, amine, and hydroxyl groups (Table 1). These
 288 peaks will change as a function of pH if the protonation of functional groups on the cell
 289 surface change. The peaks at 1726 and 1400 cm^{-1} (peaks a and e) are directly related to the
 290 protonation and deprotonation of carboxyl groups on the bacterial cell wall, with 1726 cm^{-1}
 291 decreasing as 1400 cm^{-1} increases following the deprotonation of the carboxyl group with
 292 increasing pH. This has been observed in other studies (e.g. Jiang et al., 2004; Ojeda et al.,
 293 2008). We observe changes in the amide I band at 1637 cm^{-1} , these changes may be related to
 294 various amounts of residual water in the cells or may be related to hydroxyl groups (Table 1).
 295 Changes in the band at 1554 cm^{-1} relate to changes in amino functional groups as well as N-H
 296 and C-N bonds in amide II in proteins. Due to the overlapping nature of the peaks for
 297 phosphate groups with methyl and carboxyl bonds and with phosphates and amines that are
 298 not proton active (ie not protonating and deprotonating on the cell surface), it is difficult to
 299 assign proton-active phosphate groups to specific bands. However, deprotonation of
 300 phosphate groups can be seen via changes in peaks at 1247, 1228, 1118, 1090, 1066, and
 301 1047 cm^{-1} .

Table 1. Assignments of important vibrational bands, compiled after Jiang et al., 2004; Parikh and Chorover, 2006, Ojeda et al., 2008

IR band	Wavenumber (cm^{-1})	Assignment
a	1726	$\nu_s\text{C=O}$ of protonated carboxylic acid groups

b	1648	stretching of C=O in amide I, associated with proteins and δ O-H of water
c	1554	N-H bending and C-N stretching in amide II, associated with proteins
d	1465	δ_{as} CH ₃ and δ_{as} CH ₂ of lipids or proteins
e	1400	ν_s COO ⁻ from carboxyl groups
f	1247/1228	ν_{as} P=O of phosphodiester/phosphate monoester phosphate/ ν_s C-O of COO ⁻ groups
g	1178	ν C-O from carbohydrates
h	1118	ν_s C-C, ν_s P-O-C, ν_{as} C-O-C from phosphate/phosphodiester and carbohydrates
i	1090	ν_s PO ₂ ⁻ and ν_s P-O-C of the phosphodiester
j	1066	Mixed vibrational modes of carbohydrates and phospholipids; ν_s PO ₂ ⁻ , δ C-O-P, ν_s C-OH, C-O-C, and
k	1047	δ (P-O-P), ν OH, δ C-O

ν_s = symmetric stretching; ν_{as} = asymmetric stretching; δ = bending

302

303 The biggest difference between the cells at each growth phase is in the death phase cells,
304 where unlike the exponential and stationary phase cells, there is little change in spectral
305 bands above pH 4 (Figure 4), specifically in the region 1100-1000 cm⁻¹. This means that the
306 most significant differences between the phases relates to death phase having significantly
307 more proton-active carboxyl groups than the other growth phases. This supports the
308 interpretation that the increase in site concentrations observed in the surface complexation
309 modelling, was due to an increase in carboxyl groups. Alginate is a class of EPS made up of
310 D-mannuronic and L-guluronic acid assembled into β -1,4-linked blocks (Sutherland, 2001),
311 and is rich in carboxyl groups. An increase in capsular EPS around the cells would explain
312 the lack of change in the spectral data in death phase above pH 4 as this would increase peaks
313 related to carboxyl groups relative to those of phosphate (increase in 1066 and 1047 cm⁻¹
314 relative to 1090 cm⁻¹). This is further supported by the increase seen in peaks at 1066 and
315 1047 cm⁻¹ as cells age from exponential to death phase, relating to an increase in EPS (Quiles
316 et al., 2010). This significant increase in carboxyl groups would drown out the differences in
317 peaks at 1066 and 1047 cm⁻¹ seen in exponential and stationary phase that would relate to

318 deprotonation of phosphate moieties. Therefore, given the results from the cell surface
319 characterisation, we would expect cells at death phase to be able to remove significantly more
320 U from solution via the increased concentrations of EPS surrounding the cells, and thereby
321 proton active groups available for U binding.

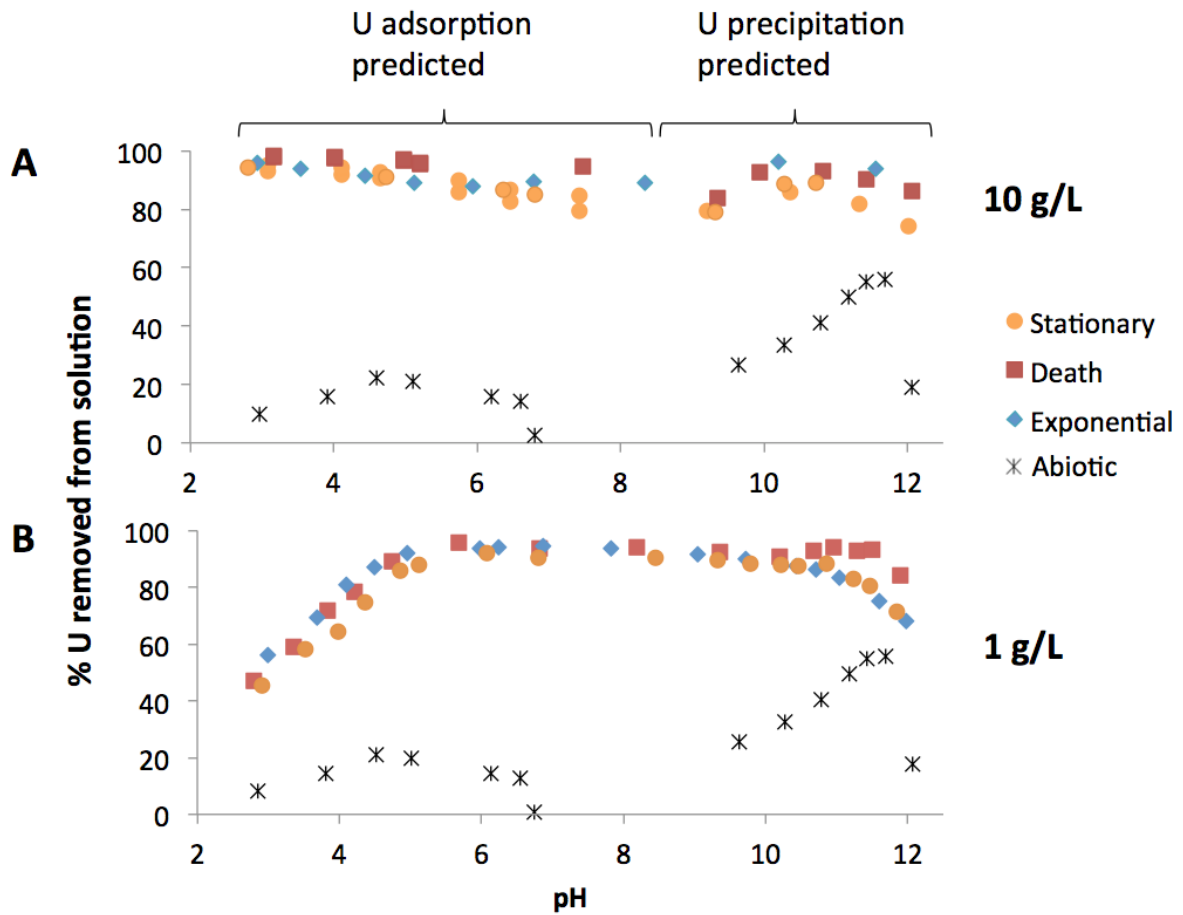
322

323 **3.2 How Growth Phase and Culture Concentration Affects Uranium Removal**

324 Uranium batch removal experiments were conducted as a function of pH for each of the
325 bacterial growth phases studied at 10 g/L and 1 g/L concentrations of bacteria in solution
326 (Figure 5 A and B, respectively). Each growth phase removed a similar percentage of U from
327 solution at a given pH. Lowering the concentration of cells in solution reduced the extent of
328 U removal from solution at pH values less than 5 and greater than 11. To test how much
329 bacteria in solution were needed for U removal, further experiments were conducted as a
330 function of bacterial concentration. There was no difference observed with respect to the
331 extent of U removed from solution as a function of growth phase, which was unexpected
332 since death phase cells had higher concentration of sites available for binding U.

333 Regardless of the differences in site density, U removal from solution did not change
334 significantly as a function of bacterial growth phase. This is different to what was seen by
335 Daughney et al. (2001), where their cells at exponential phase had significantly more sites for
336 binding than cells at stationary phase which led to increases in the extent of Cd and Fe
337 removed from solution from pH 2-8. However, this is similar to what was seen previously for
338 *P. putida* by Kenney and Fein (2011), where the presence or absence of EPS did not change
339 the extent of Cd binding to the cell walls as a function of pH.

340

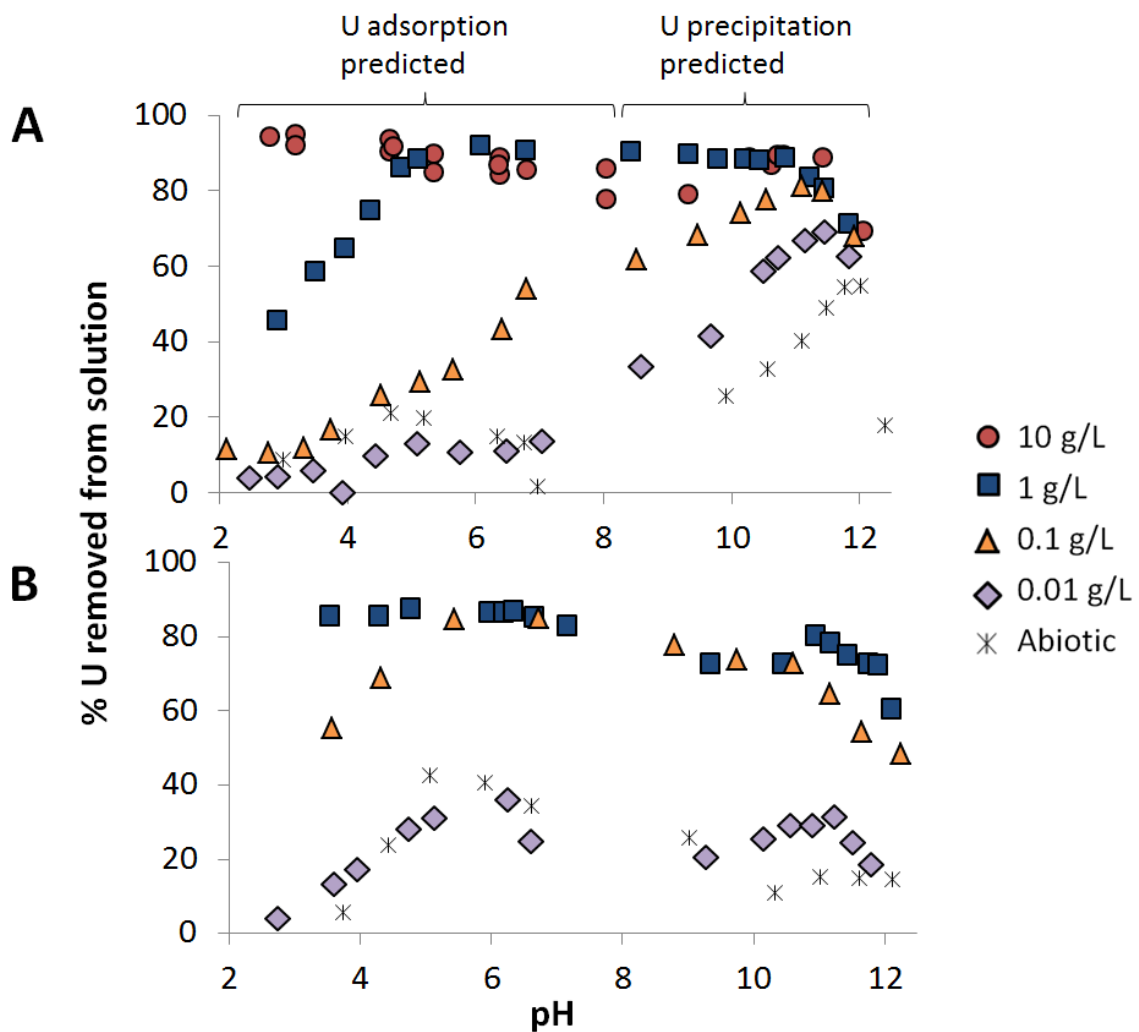


341
342

343 **Figure 5: Percentage of U removal by bacteria across all growth phases as a function of**
 344 **pH in 0.1M NaCl electrolyte solution using A) 10 g/L and B) 1 g/L wet mass of bacteria**
 345 **in solution. Error associated with analytical measurements is $\pm 5\%$.**

346 Figure 6 shows the results from the batch U removal experiments as a function of pH,
 347 bacterial culture concentration (0-10 g/L) and U concentration (10 and 1 ppm, Figure 6A and
 348 B, respectively). The bacterial concentration experiments were conducted at stationary
 349 growth phase since few changes were seen as a function of growth phase (Figure 5, see
 350 discussion above). Lowering the concentration of cells in solution lowered the extent of U
 351 removal from solution significantly at pH values lower than 8, but only slightly at pH values
 352 greater than 8. Similar trends are seen in experiments with both U starting concentrations,
 353 with decreasing U removal with decreasing concentration of cells in solution. However, the

354 extent of U removed from solution decreased significantly at lower pH values (< pH 8).
 355 Above pH 8 even the smallest concentrations of cells in solution were able to remove a
 356 significant concentration of U from solution when compared to abiotic removal. Therefore it
 357 is likely that U is adsorbed at lower pH values and precipitated at higher pH values, as was
 358 seen in abiotic mineral adsorption experiments with similar U concentrations and
 359 groundwater chemistry as seen by Kenney et al., (2017). This means that at pH values
 360 associated with trench disposal of LLW, there needs to be a significant amount of bacteria
 361 present to impact the mobility of U in solution. At the high pH values associated with
 362 cementitious disposal of LLW or ILW in a geological repository, only a small fraction of
 363 bacteria is needed to significantly increase the precipitation of U from solution.
 364



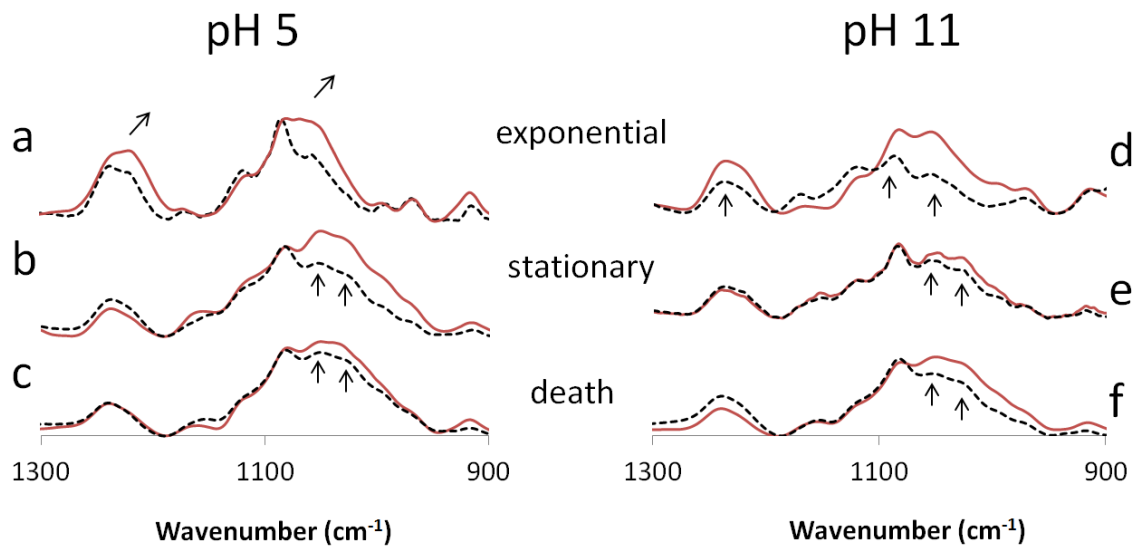
366

367 **Figure 6: Percentage of U removal by bacteria at stationary phase only, as a function**
368 **of U:bacteria ratios and pH in 0.1M NaCl electrolyte solution with initial U**
369 **concentrations of A) 10 ppm and B) 1 ppm.**

370

371 **3.3 Mechanisms of Uranium Removal**

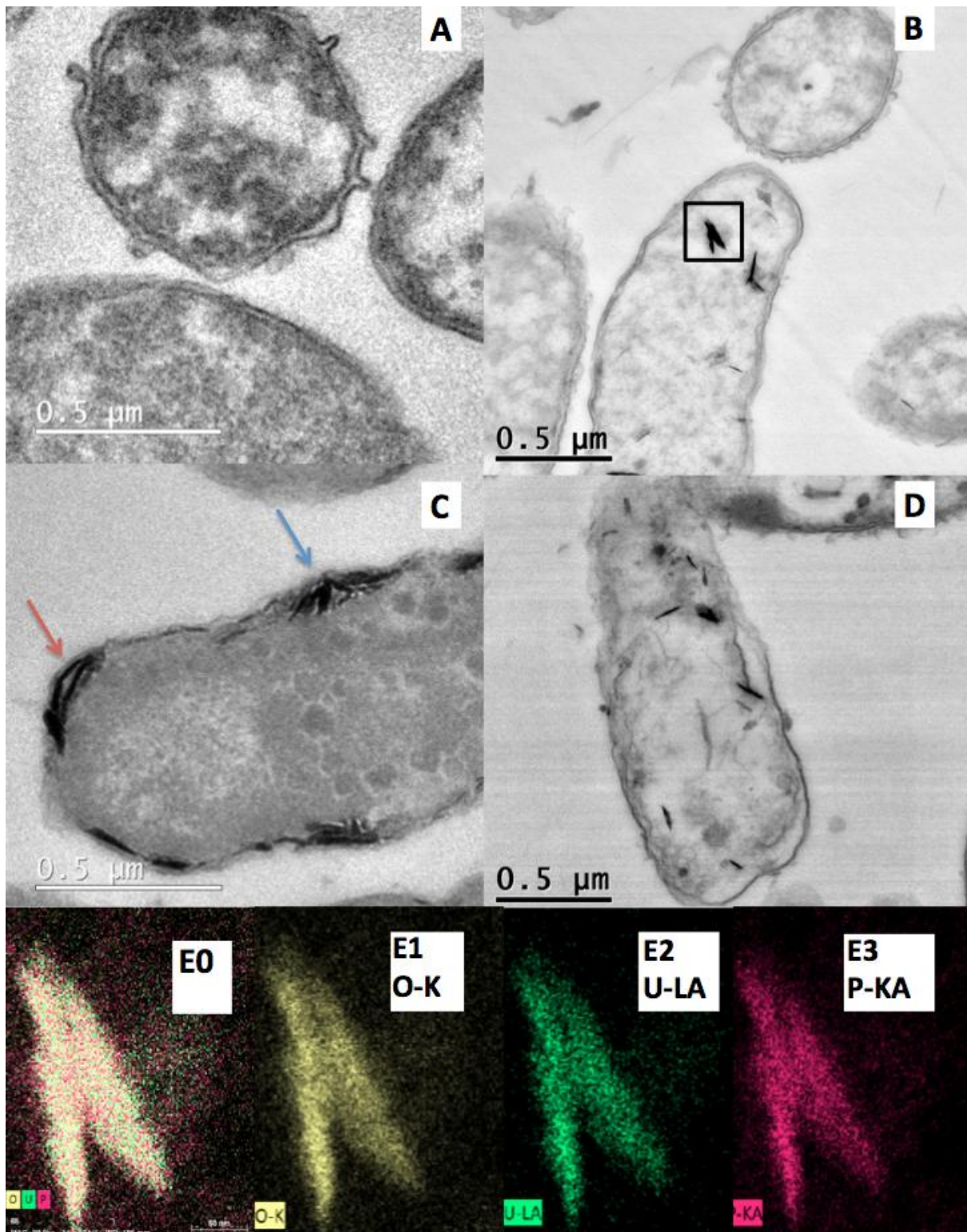
372 The mechanism of U removal from solution as a function of growth phase was examined for
373 cells with and without U using FT-IR spectroscopy (Figure 7), probing cells with and without
374 U at pH 5 and pH 11 as a function of growth phase. Unlike what was observed in the batch U
375 removal experiments, FT-IR spectroscopy (Figure 7) showed differences between the growth
376 phases. Exponential phase cells at pH 5 showed an increase in peaks at 1240 cm^{-1} and the
377 peak at 1228 cm^{-1} was shifted down to 1222 cm^{-1} , indicating adsorption of U to either the
378 phosphate or carboxyl group, as well as an shift in the peak at 1074 cm^{-1} increasing in
379 intensity and shifting to 1064 cm^{-1} , which represents mixed vibrational modes of
380 carbohydrates and phosphodiesteres. This trend was not seen in the regions where only
381 carboxyl groups were present, therefore we attribute this shift to adsorption to the phosphate
382 functional group. At pH 11 there is no shift in the spectra at 1240 cm^{-1} or 1066 cm^{-1} after the
383 addition of U, but an increase in those bands. This indicates that instead of adsorption, we
384 have the precipitation of a U-phosphate mineral. Stationary phase exhibited no shifts in their
385 spectra at 1240 cm^{-1} at pH 5 after U was reacted with the bacteria. There is an increase in
386 intensity in the peaks at 1066 and 1047 cm^{-1} likely associated with the precipitation of U
387 phosphates or carbonates, and this trend was also observed but to a lesser degree at pH 11.
388 Death phase spectra were similar to those at stationary phase, with no spectral shifts and
389 increases in bands at 1066 and 1047 cm^{-1} for cells at pH 5 and 11.



390

391 **Figure 7: FT-IR spectra of bacteria at each growth phase at pH 5 (a, exponential; b,**
 392 **stationary; and c, death phase) and 11 (d, exponential; e, stationary; and f, death phase)**
 393 **with (red lines) and without (black lines) U equilibrated for 2h with 1g/L bacteria and**
 394 **10ppm U in suspension.**

395 Precipitation of U-phosphate minerals have been seen in experiments conducted at lower pH
 396 values (pH < 6) and precipitated in the cell wall or in the cytoplasm, depending on Gram type
 397 (Beveridge et al., 1983; Merroun et al., 2011; Theodorakopoulos et al., 2015). Uranium
 398 phosphate minerals were also seen to precipitate anaerobically by Alessi et al (2014), who
 399 observed the formation of a reduced, non-crystalline uranium phosphate phase associated
 400 with biomass that showed similar increases in spectral bands between 1200-900 cm⁻¹.
 401 Therefore we would expect an uranyl phosphate precipitate to be found associated with the
 402 cells and not a carbonate species. These experiments also show that cells at pH 11 are similar
 403 in spectral changes as a function growth phase when exposed to U, however at pH 5 growth
 404 phase may play a significant role in determining the mechanism of U removal. This will be
 405 further analysed with TEM below.

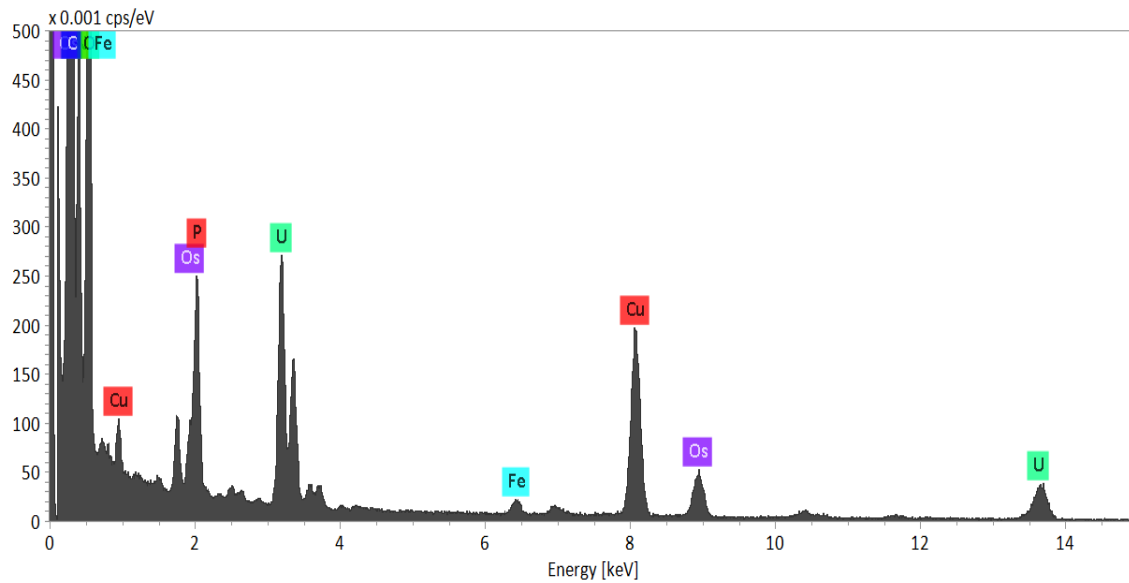


408 **Figure 8:** TEM micrographs of *P. putida* cells at exponential phase at pH 5 (A) and pH
 409 **11 (B)** and stationary phase at pH 5 (C) and pH 11 (D) with 10 ppm U. E1-E3 show
 410 corresponding EDX elemental maps of the boxed region in B, showing the distribution

411 **of O, U and P in the precipitates. E0 is the overlay (O-K, U-LA, and P-KA, combined)**
412 **elemental map.**

413 To confirm whether the differences observed in the FT-IR spectra of bacterially associated U
414 were due to adsorption or precipitation, samples from exponential and stationary phase at pH
415 5 and 11 were analysed using TEM (pH 5; Figure 8 A and C) and STEM (pH 11; Figure 8 B
416 and D), and an elemental map of a typical mineral precipitate at pH 11 was analysed using
417 STEM-EDX (Figure 8 box in B with maps E0-E3). Death phase cells were not examined
418 since the FT-IR results show little difference between spectra of cells at stationary and death
419 phase.

420 TEM data confirmed that there was a significant difference in the mechanism of U removal
421 from solution with cells various growth phase and pH conditions. In the exponential phase at
422 pH 5 (Figure 8A), there was no evidence of mineral precipitation within the cells. A
423 precipitate was found in all other cells, with a length of $0.17 \pm 0.6 \mu\text{m}$ long, based on 60
424 measurements. The cells in the exponential phase at pH 11 (Figure 8C) contained high aspect
425 ratio needle-like precipitates within the cells. EDX elemental mapping of the chevron-shaped
426 cluster of precipitates in Figure 8B (boxed region) are shown in Figures 8 E0-E3 and an
427 example of the spectra are shown in Figure 9, confirming that the precipitates are rich in
428 uranium, phosphorous and oxygen and are most probably a U-phosphate mineral.
429 Precipitates with a similar morphology were also seen inside the cells in the stationary phase
430 at both pH 5 and 11 (Figure 8 C and D, respectively) but the distribution of the precipitates
431 was markedly different. Point EDX analysis of precipitates show U/P ratios of between 0.6
432 and 2.4, which is likely to be related to the variable P concentrations found in the cell, as the
433 concentration of P will differ between the cytoplasm, ribosomes, nucleoid, and cell wall
434 (Madigan and Martinko, 2006)



435

436 **Figure 9: Example of EDX spectra from boxed region in Figure 8.**

437 Clusters and individual precipitates were aligned with their long axis parallel to, and just
 438 inside the cell wall of the cells in the stationary phase at pH 5 (red arrow, Figure 8C) with a
 439 population of precipitates oriented with a higher contact angle to the cell wall (blue arrow,
 440 Figure 8C). In contrast, in the precipitates associated with cells at exponential and stationary
 441 phase at pH 11 were distributed within the cell interior and separated from the cell wall. The
 442 cell wall of Gram-negative bacteria are rich in lipopolysaccharides and membrane proteins,
 443 which have many phosphate moieties, and would act as a nucleation point for U-phosphate
 444 minerals. Merroun et al. (Merroun et al., 2011) found that cells grown to late exponential
 445 phase were able to precipitate U from a supersaturated U solution at pH 2-4.5 both in the cell
 446 wall and within their Gram-negative cells. In our study, the observed differentiation between
 447 precipitates occurring in the cell wall and those occurring within the cell may relate to the
 448 rupturing of cells at high pH, allowing for the U to enter the cells and precipitate with the P
 449 made available via lysis. Cells at pH 5 are not lysed and therefore the U remains at the cell
 450 wall for cells at stationary phase. As cells age from exponential phase to stationary phase, the
 451 integrity of the outer membrane may break down allowing for entry of U into the periplasmic

452 space and precipitate using the phosphate within the double membrane. Ohnuki et al. (2005)
453 observed H-autunite, ($\text{HUO}_2\text{PO}_4 \cdot 4\text{H}_2\text{O}$) precipitated at ruptured regions of *Saccharomyces*
454 *cerevisiae* cells grown with excess P. This is similar to our observations in solutions of pH 11
455 cells, where the ruptured cells allow for the U to enter the cell and scavenge intracellular P,
456 whereas at pH 5 the U only enters the double membrane of *P. putida*.

457 In the context of a GDF (G, post-closure, U(VI) may still be present due to the reoxidation of
458 U(IV) in the presence of bacteria, bicarbonate, Fe, and Mn, all things that will likely be in the
459 subsurface environment. A GDF would have a different bacterial population than the
460 surrounding host rock since foreign bacteria would be introduced during the engineering and
461 operational phases, however the bacteria would likely evolve their population based on the
462 high pH of the cement-equilibrated groundwater. Therefore the bacteria directly surrounding
463 the GDF would likely be alkaliphilic extremophile bacteria, and as pH decreases away from
464 the GDF the pH would lower to background levels, allowing neutralophilic bacteria to
465 flourish. Kenney and Fein (2011) found that acidophilic, alkaliphilic, and neutralophilic
466 bacteria rely on the same functional groups to remove the same extent of protons and metal
467 from solution across a pH range from 1.8-11.5. Therefore, since the cells in our study
468 passively remove U from solution via precipitation nucleated at the phosphate moieties in the
469 cell wall, or in the cytoplasm, a wide range of bacteria in the subsurface should be able to
470 remove U(VI) from solution in the same manner as in our study. The differences in our study
471 may arise given that our cells were neutralophiles, and would break down at high pH, which
472 led to precipitation of uranyl phosphates within the cells. If the cells in solution at high pH
473 were alkaliphilic bacteria, their cell walls would remain more stable and we would see the
474 same type of cell wall-bound precipitation as in our pH 5 experiments.

475

476

477 **Conclusions**

478 In this study, we investigated how growth phase and culture concentration of *P. putida*
479 affected the removal of U from solution in the pH range between 2 and 12, under aerobic
480 conditions. To do this we first characterised how the bacterial cells changed as a function of
481 growth phase. This was completed via the surface complexation modelling of potentiometric
482 titration data. We found that exponential and stationary growth phase had similar acidity
483 constants and site densities, while death phase cells exhibited higher site densities for the
484 first three surface sites identified. This increase in site density was reflected in the FT-IR
485 spectroscopic results, where death phase showed a higher concentration of carboxyl groups
486 and the lack of spectral changes with pH, and was due to an increase in capsular EPS.

487 However the presence of EPS did not affect the extent of U removed from solution; the same
488 extent of U was removed from solution at any given pH value between 2-12 regardless of
489 growth phase. Lowering the culture concentration of *P. putida* in solution did have a strong
490 effect on the amount of U removed from solution, with decreasing U removed from solution
491 with decreasing cells in suspension at pH values less than 8. Above 8 there was only a slight
492 decrease in the extent of U removed from solution since even the smallest concentrations of
493 cells in solution studied was able to precipitate significantly more U than the abiotic system.
494 FT-IR spectroscopy coupled with TEM/STEM-EDS showed that the mechanism of U
495 removal from solution was highly affected by pH and growth phase. During the exponential
496 phase, cells adsorbed U at low pH and precipitated U intracellularly at high pH, whereas
497 during the stationary phase, cells precipitated a U-phosphate in the cell membrane at low pH
498 and intracellularly at high pH. Therefore, the form of U removed from solution may change
499 drastically depending on the growth phase of the bacteria in solution.

500 **Acknowledgements**

501 We acknowledge the Natural Environment Research Council, Radioactive Waste
502 Management Limited, and Environment Agency for the funding received for this project
503 through the Radioactivity and the Environment (RATE) programme. We thank Prof. Mark
504 Sephton for the use of his FT-IR spectrometer in the Department of Earth Science and
505 Engineering at Imperial College London, and Dr. Simon Norris from RWM and Dr. Gavin
506 Thomson for their insights in writing this manuscript.

507

508 **References**

- 509 Azam, T.A., Iwata, A., Nishimura, A., Ueda, S., Ishihama, A., 1999. Growth phase-dependent variation
510 in protein composition of the Escherichia coli nucleoid. *Journal of Bacteriology*, 181(20):
511 6361-6370.
- 512 Barkleit, A., Moll, H., Bernhard, G., 2009. Complexation of uranium(VI) with peptidoglycan. *Dalton*
513 *Transactions*(27): 5379-5385.
- 514 Bots, P. et al., 2014. Formation of Stable Uranium(VI) Colloidal Nanoparticles in Conditions Relevant
515 to Radioactive Waste Disposal. *Langmuir*, 30(48): 14396-14405.
- 516 Bourbon, X., Toulhoat, P., 1996. Influence of organic degradation products on the solubilisation of
517 radionuclides in intermediate and low level radioactive wastes. *Radiochimica Acta*, 74: 315-
518 319.
- 519 Conti, E., Flaibani, A., Oregon, M., Sutherland, I.W., 1994. Alginate from *Pseudomonas-Fluorescens*
520 and *P-Putida* - Production and Properties. *Microbiology-Uk*, 140: 1125-1132.
- 521 Daughney, C.J., Fowle, D.A., Fortin, D.E., 2001. The effect of growth phase on proton and metal
522 adsorption by *Bacillus subtilis*. *Geochimica Et Cosmochimica Acta*, 65(7): 1025-1035.
- 523 Dunham-Cheatham, S. et al., 2011. The effects of non-metabolizing bacterial cells on the
524 precipitation of U, Pb and Ca phosphates. *Geochimica Et Cosmochimica Acta*, 75(10): 2828-
525 2847.
- 526 Felten, J. et al., 2015. Vibrational spectroscopic image analysis of biological material using
527 multivariate curve resolution-alternating least squares (MCR-ALS). *Nature Protocols*, 10(2):
528 217-240.
- 529 Fletcher, M., 1977. Effects of Culture Concentration and Age, Time, and Temperature on Bacterial
530 Attachment to Polystyrene. *Canadian Journal of Microbiology*, 23(1): 1-6.
- 531 Fowle, D.A., Fein, J.B., Martin, A.M., 2000. Experimental study of uranyl adsorption onto *Bacillus*
532 *subtilis*. *Environmental Science & Technology*, 34(17): 3737-3741.
- 533 Francis, A.J. et al., 2004. Uranium association with halophilic and non-halophilic bacteria and
534 archaea. *Radiochimica Acta*, 92(8): 481-488.
- 535 Gad, F., Zahra, T., Hasan, T., Hamblin, M.R., 2004. Effects of growth phase and extracellular slime on
536 photodynamic inactivation of gram-positive pathogenic bacteria. *Antimicrobial Agents and*
537 *Chemotherapy*, 48(6): 2173-2178.

- 538 Gorman-Lewis, D., Elias, P.E., Fein, J.B., 2005. Adsorption of aqueous uranyl complexes onto *Bacillus*
539 *subtilis* cells. *Environmental Science & Technology*, 39(13): 4906-4912.
- 540 Green, E.R., Meccas, J., 2016. Bacterial Secretion Systems: An Overview. *Microbiol Spectr*, 4(1).
- 541 Heinrich, H.T.M., Bremer, P.J., McQuillan, A.J., Daughney, C.J., 2008. Modelling of the acid-base
542 properties of two thermophilic bacteria at different growth times. *Geochimica Et*
543 *Cosmochimica Acta*, 72(17): 4185-4200.
- 544 Janssen, M.J.F.W., Koorengel, M.C., de Kruijff, B., de Kroon, A.I.P.M., 2000. The
545 phosphatidylcholine to phosphatidylethanolamine ratio of *Saccharomyces cerevisiae* varies
546 with the growth phase. *Yeast*, 16(7): 641-650.
- 547 Jiang, W. et al., 2004. Elucidation of functional groups on gram-positive and gram-negative bacterial
548 surfaces using infrared spectroscopy. *Langmuir*, 20(26): 11433-11442.
- 549 Kelly, S.D. et al., 2002. X-ray absorption fine structure determination of pH-dependent U-bacterial
550 cell wall interactions. *Geochimica Et Cosmochimica Acta*, 66(22): 3855-3871.
- 551 Kenney, J.P.L., Kirby, M.E., Cuadros, J., Weiss, D.J., 2017. A conceptual model to predict uranium
552 removal from aqueous solutions in water-rock systems associated with low-and
553 intermediate-level radioactive waste disposal. *Rsc Advances*, 7(13): 7876-7884.
- 554 Kenney, J.P.L., Fein, J.B., 2011. Cell Wall Reactivity of Acidophilic and Alkaliphilic Bacteria Determined
555 by Potentiometric Titrations and Cd Adsorption Experiments. *Environ. Sci. Technol.*, 45,
556 4446-4452.
- 557 Lalonde, S.V., Smith, D.S., Owttrim, G.W., Konhauser, K.O., 2008. Acid-base properties of
558 cyanobacterial surfaces I: Influences of growth phase and nitrogen metabolism on cell
559 surface reactivity. *Geochimica Et Cosmochimica Acta*, 72(5): 1257-1268.
- 560 Leone, L. et al., 2007. Modeling the acid-base properties of bacterial surfaces: A combined
561 spectroscopic and potentiometric study of the gram-positive bacterium *Bacillus subtilis*.
562 *Environmental Science & Technology*, 41(18): 6465-6471.
- 563 Li, X.L. et al., 2016. Bioaccumulation characterization of uranium by a novel *Streptomyces*
564 *sporoverrucosus* dwc-3. *Journal of Environmental Sciences*, 41: 162-171.
- 565 Liang, X.J., Csetenyi, L., Gadd, G.M., 2016. Uranium bioprecipitation mediated by yeasts utilizing
566 organic phosphorus substrates. *Applied Microbiology and Biotechnology*, 100(11): 5141-
567 5151.
- 568 Liu, Y.X. et al., 2016. Cell surface acid-base properties of the cyanobacterium *Synechococcus*:
569 Influences of nitrogen source, growth phase and N:P ratios. *Geochimica Et Cosmochimica*
570 *Acta*, 187: 179-194.
- 571 Liu, Y.X. et al., 2015. Cell surface reactivity of *Synechococcus* sp PCC 7002: Implications for metal
572 sorption from seawater. *Geochimica Et Cosmochimica Acta*, 169: 30-44.
- 573 Maassen, C.B.M., Boersma, W.J.A., van Holten-Neelen, C., Claassen, E., Laman, J.D., 2003. Growth
574 phase of orally administered *Lactobacillus* strains differentially affects IgG1/IgG2a ratio for
575 soluble antigens: implications for vaccine development. *Vaccine*, 21(21-22): 2751-2757.
- 576 Madigan, M., Martinko, J. (Eds.), 2006. *Brock Biology of Microorganisms*, 11th ed.
577 Prentice. ISBN: 0131443291
- 578 Marshall, K.C., 1986. Adsorption and Adhesion Processes in Microbial-Growth at Interfaces.
579 *Advances in Colloid and Interface Science*, 25(1): 59-86.
- 580 Merroun, M.L. et al., 2011. Bio-precipitation of uranium by two bacterial isolates recovered from
581 extreme environments as estimated by potentiometric titration, TEM and X-ray absorption
582 spectroscopic analyses. *Journal of Hazardous Materials*, 197: 1-10.
- 583 Ojeda, J.J., Romero-Gonzalez, M.E., Bachmann, R.T., Edyvean, R.G.J., Banwart, S.A., 2008.
584 Characterization of the cell surface and cell wall chemistry of drinking water bacteria by
585 combining XPS, FTIR spectroscopy, modeling, and potentiometric titrations. *Langmuir*, 24(8):
586 4032-4040.
- 587 Pedersen, K., Ekendahl, S., 1990. Distribution and activity of bacteria in deep granitic groundwaters
588 of southeastern sweden. *Microbial Ecology*, 20(1): 37-52.

- 589 Quiles, F., Humbert, F., Delille, A., 2010. Analysis of changes in attenuated total reflection FTIR
590 fingerprints of *Pseudomonas fluorescens* from planktonic state to nascent biofilm state.
591 *Spectrochimica Acta Part a-Molecular and Biomolecular Spectroscopy*, 75(2): 610-616.
- 592 Rolfe, M.D. et al., 2012. Lag Phase Is a Distinct Growth Phase That Prepares Bacteria for Exponential
593 Growth and Involves Transient Metal Accumulation. *Journal of Bacteriology*, 194(3): 686-
594 701.
- 595 Sheng, L., Fein, J.B., 2013. Uranium adsorption by *Shewanella oneidensis* MR-1 as a function of
596 dissolved inorganic carbon concentration. *Chemical Geology*, 358: 15-22.
- 597 Snider, C.A., Voss, B.J., McDonald, W.H., Cover, T.L., 2016. Growth phase-dependent composition of
598 the *Helicobacter pylori* exoproteome. *Journal of Proteomics*, 130: 94-107.
- 599 Sutherland, I.W., 2001. Biofilm exopolysaccharides: a strong and sticky framework. *Microbiology-Uk*,
600 147: 3-9.
- 601 Wan, J., Tokunaga, T.K, Brodie, E., Wang, Z., Zheng, Z., Herman, D., Hazen, T.C., Firestone, M.K.,
602 Sutton, S.R. 2005. Reoxidation of Bioreduced Uranium under Reducing Conditions. *Environ.*
603 *Sci. Technol.*, 39 (16): 6162-6169
604

605

606 **Graphical Abstract**

